Influence of Processing on Ethylene Propylene Block Copolymers (II): Fracture Behavior

J. Gamez-Perez, P. Muñoz, O. O. Santana, A. Gordillo, M. Ll. Maspoch

Centre Català del Plàstic, Universitat Politècnica de Catalunya, C. Colom 114, 08222, Terrassa, Spain

Received 14 July 2004; accepted 3 June 2005
DOI 10.1002/app.23024
Published online 2 June 2006 in Wiley InterScience (www.interscience.wiley.com).

ABSTRACT: The present work investigates the relationships between the microstructural state and fracture properties in commercial polypropylene-based materials. In this case an isopolypropylene homopolymer and three ethylene propylene block copolymers (EPBC) with different ethylene content (EC) have been studied. A variety of morphologies were obtained by a combination of several processing methods (injection molding, injection molding-annealing, and compression molding) and thickness. Fracture behavior of deeply double-edged notched specimens was evaluated by scanning electron microscopy (SEM) and by the essential work of fracture (EWF) method, analyzing the influence of processing, thickness (t), EC, and orientation respect to melt flow direction (MD and TD). The testing direction and EC are the most relevant variables that affect the ability of the crack tip to deform plastically during the crack propagation, determining the final fracture behavior. The fracture parameters obtained with the EWF method, specific EWF, w_e, and plastic item, βw_p, have proved to be very sensitive to the processing induced morphology, finding interesting relationships between such morphologies (characterized by crystallinity index, orientation level, and skin/core ratio) and the fracture parameters of the plaques. © 2006 Wiley Periodicals, Inc. J Appl Polym Sci 101: 2714–2724, 2006

Key words: polypropylene block copolymers; essential work of fracture; structure-properties relations; skin–core morphology; injection molding

INTRODUCTION

Ethylene propylene block copolymers (EPBC) are widely used in different industrial applications,[1] where it is desirable to obtain good combination of properties between polyethylene and polypropylene (PP). Some of these applications search a higher impact resistance, as in the automotive industry, and/or the preservation of ductile behavior of a piece at low service temperatures, as in the case of some food containers.

In a previous work,[2] it has been studied the influence of thickness, ethylene content (EC), and processing method on the microstructure and tensile behavior of thin plaques obtained by injection and compression molding. The use of an additional annealing step after injection molding was considered to broaden the spectrum of morphologies present in the study and also because commercial EPBC articles may be exposed during their service life to high temperature environmental conditions, in which some secondary crystallization phenomena can take place, affecting their crystalline structure.

The purpose of the present work is to investigate on the influence that the morphology has on the fracture properties of EPBC plaques obtained with different processing methods, thickness, and EC.

EXPERIMENTAL

Materials

Four commercial PP-based materials, one isopolypropylene homopolymer (H0) and three EPBC with 5.5, 7.4, and 12% in weight EC (determined by FTIR), from now on C1, C2, and C3, respectively, have been employed in this work. The grades were chosen with the most similar melt flow indexes available, to use the same processing conditions with all of them. All the materials, which have been the object of previous works of our group,[2–5] were kindly supplied by Basell (Barcelona, Spain).

Processing

The raw materials were received as pellets and processed by injection-molding machine Mateu and Solé 900 Tm (Barcelona, Spain) to obtain thin plaques of different thickness (t = 1, 2, and 3 mm), as pictured in Figure 1. The barrel temperatures (not considering the feeding zone) ranged from 200 to 230°C and the temperature in the nozzle was 250°C. The molds were maintained at 28°C by means of a cooling circuit filled

Correspondence to: M. L. Maspoch.
Contract grant sponsor: MCYT; contract grant number: MAT 2000–1112.

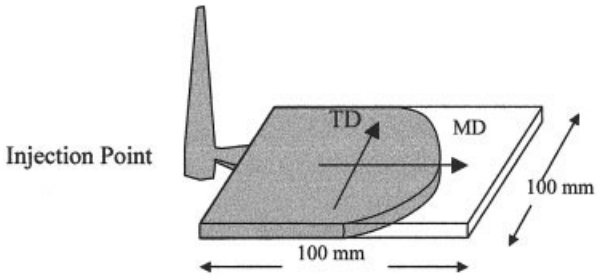

Figure 1 Scheme of an injected plaque indicating the melt flow direction (MD) and the transversal direction (TD).

with water. The three molds were provided with a fan-gate entrance of thickness, a half of that of the plaque.

Additionally, some plaques were subjected to an annealing process at 130°C during 2.5 h. Within this time the annealing was considered complete.

On the other hand, plaques of all materials were obtained with a hot plate hydraulic press at 180°C and 45 bars in two nominal thickness (1 and 2 mm). According to the material, thickness, and processing method, the following code has been assigned to the plaques: material-thickness, processing, IM for injection molding, IMA for injection and annealing, and CM for compression molding (i.e., the sample named "C2–1mm IMA," represents the plaques of material C2, 1mm thick and obtained by injection molding—annealing). The direction in which the plaques have been tested has been specified as MD or TD (melt flow direction and transversal to the melt flow, respectively), as shown in Figure 1.

Structure characterization

The morphological and structural characterization was carried out using polarizing light microscopy (PLM), differential scanning calorimetry (DSC), and wide angle X-ray scattering (WAXS). These results have been already reported in a previous work[2] and we will refer to them if necessary to discuss their influence on the fracture behavior. A summary of the morphological properties from the mentioned paper can be found in Table I.

Fracture behavior

To characterize properly the fracture properties, the essential work of fracture (EWF) technique was applied. Deeply double-edged notched specimens (DDENT), as depicted in Figure 2, were prepared and tested in tension loading at a nominal rate of 2 mm/min and room temperature (23°C) in both MD and TD directions.

The fractographic analysis was carried out after gold-coating the fractured surfaces with scanning electron microscopy (SEM), using a JEOL JSM 6400 (Jeol Europe, France).

The EWF method was initially developed by Cotterell and Reddel,[6] following Broberg's work,[7] for the characterization of ductile fracture in metal sheets. Afterwards, it was applied with success to plastic film and sheets,[8] and in the last decade multiple works have shown the convenience of employing the EWF method to characterize fracture properties of polymer thin sheets and films.[9–14] Also, there have been many contributions to develop the technique in their experimental details[15–20] as well as to understand the influence among the fracture parameters thus obtained and the microstructure and morphology of the fractured materials.[5,10,21]

The EWF method is based on the partition of the energy consumed during the postyielding fracture of a precracked specimen, W_f, where two distinct (inner and outer) zones can be observed (see Fig. 2). The

TABLE I
Summary of the Morphological Characterization of the Plaques

Material	A_{110}	χ_c	t_s (μm)
H0–1mm CM	0.56	0.82	—
H0–1mm IM	0.96	0.77	249
H0–1mm IMA	0.97		276
H0–2mm CM	0.58	0.82	—
H0–2mm IM	0.80	0.77	227
H0–2mm IMA	0.83	—	206
H0–3mm IM	0.58	0.73	196
H0–3mm IMA	0.66	—	168
C1–1mm CM	0.58	0.72	—
C1–1mm IM	0.95	0.59	313
C1–1mm IMA	0.97	0.68	293
C1–2mm CM	0.54	0.73	—
C1–2mm IM	0.89	0.63	308
C1–2mm IMA	0.90	0.69	319
C1–3mm IM	0.69	0.62	233
C1–3mm IMA	0.76	0.69	228
C2–1mm CM	0.52	0.69	—
C2–1mm IM	0.88	0.53	148
C2–1mm IMA	0.91	0.57	161
C2–2mm CM	0.51	0.64	—
C2–2mm IM	0.74	0.57	182
C2–2mm IMA	0.76	0.64	186
C2–3mm IM	0.58	0.58	220
C2–3mm IMA	0.62	0.59	207
C3–1mm CM	0.54	0.56	—
C3–1mm IM	0.79	0.51	130
C3–1mm IMA	0.89	0.57	131
C3–2mm CM	0.52	0.58	—
C3–2mm IM	0.70	0.50	232
C3–2mm IMA	0.72	0.57	229
C3–3mm IM	0.58	0.50	206
C3–3mm IMA	0.64	0.57	203

A_{110} determined by WAX in the skin.
χ_c determined by DSC in the core.
t_s determined by PLM in the middle of the plaques.

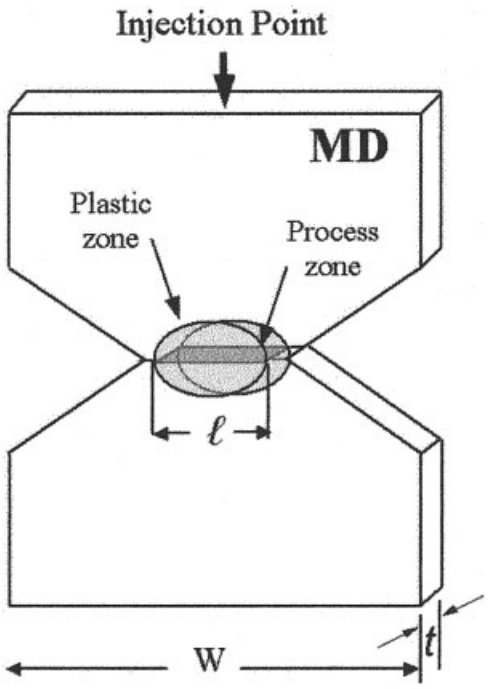

Figure 2 DDENT specimen used for the fracture characterization (EWF method). The essential work is related to the fractured surface (process zone) and the nonessential work corresponds to the plastic zone.

inner zone, also called the process zone, is where the real fracture process takes place with the formation of two new surfaces. The energy associated with it, the EWF (W_e) is proportional to the ligament section, ℓt. In the outer zone, also called the plastic zone, the energy involved is the non-EWF or plastic work (W_p), which is employed basically in plastic deformation and other dissipative process. The work consumed in this zone is proportional to the volume of the deformed region.

These concepts lead to the following expression:

$$W_f = W_e + W_p = w_e \ell t + \beta w_p \ell^2 t \qquad (1)$$

Where w_e is the specific EWF (per unit ligament area), w_p, specific non-EWF (per unit volume), ℓ **ligament length,** t, specimen thickness, and β is plastic zone shape factor. The EWF is in theory a material property for a given sheet thickness, while the nonessential depends on other parameters such as the geometry of the specimen tested or the testing rate.

Dividing both terms of the eq. (1) by the ligament section, ℓt, the specific work of fracture, w_f, can be expressed as:

$$w_f = W_f/(\ell t) = w_e + \beta w_p \ell \qquad (2)$$

According to this equation, the plot of w_f as a function of ℓ should be a linear relation, whose intercept with the y-axis and slope would give w_e and βw_p, respectively. Thus, the experimental technique consists in testing specimens with different ligament lengths, registering W_f for each one, as the total area under the force–displacement curve of the test. Then, w_e and βw_p can be calculated from the best-fit regression line of the w_f *vs.* ℓ diagram.

The specific essential work, w_e is in theory a material constant dependent only on thickness and equivalent to J_{IC}[9], which has also been supported experimentally by different authors.[10,22,23] However, the EWF method compared with the J-Integral procedure presents simplicity and applicability to thinner specimens as its experimental advantages.

According to the European Structural Integrity Society (ESIS) EWF protocol,[24] some restrictions on ligament length (ℓ) for DDENT specimens must be considered:

$$MAX(3t, 5\ mm) < \ell < W/3 \qquad (3)$$

Where W is the width of the DDENT specimen. The lower limit is to guarantee that all the samples are under the same state of tension (plane stress) and no sample is tested under mixed mode or plane strain states. Since eq. (3) can only be applied under truly plane stress fracture, Hill's criterion[25] can be used to verify this argument. The upper limit is intended to avoid edge effects on the fracture, although some authors have reported that this value is too conservative since they can obtain good linear regressions beyond the $W/3$ value.[11,17,20]

Additionally, there are other prerequisites that must be accomplished to apply the EWF method properly:

(a) The ligament must be fully yielded prior to crack propagation.
(b) The crack propagation must be steady.
(c) There must be a common geometry of fracture for all ligament lengths, visible in the self-similarity of the curves in Load–displacement (L-d) diagrams.

Since the notch quality has proved to affect strongly the EWF results,[24] all notches were sharpened with a fresh razor blade before testing.

RESULTS AND DISCUSSION

All the obtained results are summarized in Table II. To illustrate the most significant trends found within the data, selected diagrams will be represented to complete the text discussions.

Types of fracture

When the DDENT specimens were tested, different types of fracture could be observed. We found a wide spectrum of ductility of the crack tip during the frac-

TABLE II
Level of Ductility (LD) and Fracture Parameters (EWF method) Obtained for the Plaques

		H0		C1			C2			C3		
	LD	w_e (kJ/m^2)	βw_p (MJ/m^3)	LD	w_e (kJ/m^2)	βw_p (MJ/m^3)	LD	w_e (kJ/m^2)	βw_p (MJ/m^3)	LD	w_e (kJ/m^2)	βw_p (MJ/m^3)
1mm CM	−1			0	36±3	6.6±0.3	0	15±4	5.7±0.4	0	6±2	1.3±0.2
1mm IM MD	+1	123±30	21±2	+2	380±60	37±4	+2	210±20	13±1	+1	32±5	12.1±0.3
1mm IM TD	−2			0	17±2	6.5±0.2	0	26±2	4.5±0.1	0	21±1	2.0±0.1
1mm IMA MD	+1	210±90	37±8	+2	250±40	37±3	+1	90±10	18.1±0.8	0	41±2	9.7±0.1
1mm IMA TD	−2			0	20±2	5.5±0.2	0	19±1	3.4±0.1	0	15±1	1.7±0.1
2mm CM	−1			0	32±7	6.4±0.7	0	13±4	5.4±0.4	0	13±1	1*±0.1
2mm IM MD	+2	126±48	17±3	+2	103±14	26±0.9	+1	44±9	13.5±0.6	0	25±1	6.3±0.1
2mm IM TD	−1			0	22±4	7.3±0.3	0	39±2	5.4±0.1	0	22±2	3.7±0.1
2mm IMA MD	+1	28±17	15±2	+1	85±11	24.6±0.8	0	45±3	9.4±0.2	0	30±2	4.8±0.1
2mm IMA TD	−1			0	30±4	5.6±0.3	0	35±2	4.6±0.1	0	26±1	2.6±0.1
3mm IM MD	−1			+1	77±14	14.4±0.8	0	34±3	8.1±0.2	0	32±2	3.5±0.1
3mm IM TD	−1			0	22±3	7.8±0.2	0	36±3	5.3±0.2	0	28±2	3.4±0.1
3mm IMA MD	−1			0	26±7	13.2±0.6	0	35±2	7.1±0.1	0	27±1	3.1±0.1
3mm IMA TD	−1			0	34±3	6.2±0.2	0	27±1	5.5±0.1	0	23±1	2.8±0.1

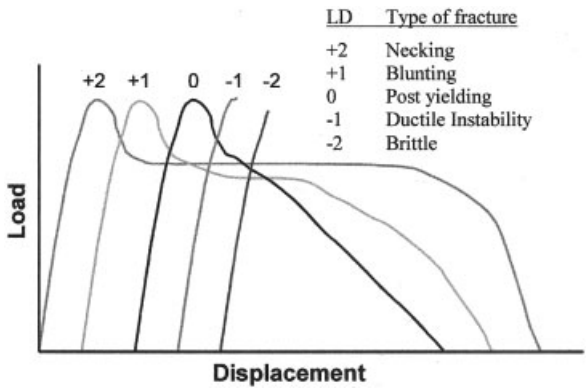

Figure 3 Classification of the different types of fracture found in PP-based materials on five levels of ductility (LD), based upon the load–displacement curves and the applicability of the EWF method.

ture process, being the limit cases the 1mm H0 injected-annealed plaque tested in the TD direction (H0–1mm IMA TD), which showed brittle behavior, and the C1–1mm IM tested in MD, which showed an extreme blunting of the notches. Such differences were revealed on the load *vs.* displacement curves and their evaluation allowed a classification of the different fracture behaviors on five levels of ductility (LD).[3,5] A scale of ductility can be assigned to these levels in terms of applicability of the EWF method as shown in Figure 3. The negative values correspond to fracture types not ductile enough and the positive ones too ductile. The "brittle" one (LD = −2) corresponds to fast crack propagation before yielding of the ligament area. Fractured DDENT specimens show small cracks against the light above the fractured section. In the ones which fail with "ductile instability" (LD = −1), the crack starts to deform plastically, when at a certain point the elastic energy stored concentrated in the tips reaches a critical value, causing an unstable crack propagation and sudden rupture. The difference between brittle and ductile instability can be assigned on postmortem specimens by the whiteness of the extremities of the ligament, which indicates the occurrence of plastic deformation identifying the latter case.

The fracture types "necking" (LD = +2) and "blunting" (LD = +1) are characterized by an extensive plastic deformation of the crack tip, which avoids steady crack propagation. In the cases named "necking" (LD = +2), the DDENT specimens show no crack propagation in the yielded ligament area, which continues to deform plastically, behaving almost like a tensile specimen and resulting in a neck formation. In the cases classified as "blunting" (LD = +1), discontinuities on the load *vs.* displacement curves are found in many cases because of blunting of the crack tip. Both types of fracture can be considered as two degrees of the same phenomenon. The elongation at break of the fractured DDENT specimens can make a

distinction between "blunting" and "necking" cases, finding lower values in the "blunting" than in the "necking" ones. It must be said that differentiation whether a fracture type could be considered as blunting or necking according to this criteria is rather subjective and it does not make a difference to the purposes of this work.

Most of the specimens showed what we called post-yielding (LD = 0) fracture behavior, which fulfils all the necessary prerequisites for applying the EWF method, previously described.

The fracture behavior of all specimens, described by the ductility level, is shown in Table II. It can be observed that the presence of ethylene prevents the brittle behavior and ductile instability that appears in the homopolymer (H0) material. This influence of the EC has been already discussed in previous works.[3–5] It is also noticeable that blunting (and necking) phenomena is present only in the injected plaques tested along the MD direction.

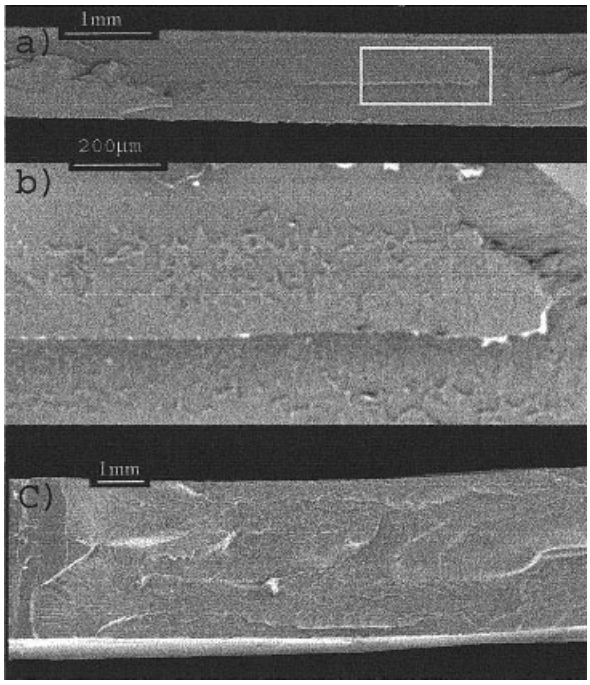

Figure 4 SEM micrographs nonductile types of fracture: (a) brittle (H0–1mm TD), (b) detail of the patch patterns, (c) ductile instability (H0–3mm TD).

SEM fractography

A more detailed analysis of the aspect of the fracture surface was possible observing the images obtained by SEM. It has been noticed that there is a correspondence between the classification made upon the load–displacement curves and the appearance of the fractured surfaces.

Brittle fracture behaviors

In Figure 4(a) SEM image of a postmortem sample of H0–1mm IM TD is shown. Such a fracture behavior, described as "brittle," shows a rather smooth surface. In addition to the small cracks visible against the light in the plastic zone, the patch patterns revealed by SEM (Fig. 4(b)) indicate that the main deformation mechanism was probably crazy.

The specimens that broke with ductile instability presented much irregular fractured surface than did the previous ones. It is noticeable that multiple cracks were originated at the failure of the material and no patch patterns were found (Fig. 4(c)).

In the case of H0–2mm IMA TD isolated patch patterns were found, although the aspect of the fractured surface looked more like the ones that failed with ductile instability.

Ductile fracture behaviors

In Figure 5, representative SEM microfotographs of the three types of ductile fracture can be found. In the "post yielding" cases (a, c, d, h, and i), the aspect of the fractured surfaces is uniform, from the notches to the center. There, different textures of the surface can be seen, depending on the material (b, f, and h) and testing direction (a, b and d, e). In the necking (b) and blunting cases (e, f, and g) a decohesion of the skin as well as some curling at the center of the fractured zone can be found. Near the notches, it can be seen that the fractured surface goes out of the ligament section, invading the plastic zone. In the cases defined as necking (b) the formation of fibers can be also appreciated.

To see the influence of the EC, a series of 2mm IM specimens fractured along the MD direction (b, f, and h) is shown in Figure 5. It can also be seen that an increase of EC in the injection-molded plaques tested along the MD direction comes with a reduction on the fracture ductility level (LD). This observation could seem contradictory at first sight, because the presence of the polyethylene should not imply any restriction to the plastic deformation; especially since the polyethylene chains are not as stiff as the PP ones. In previous works of our group, carried on thin films of the same materials,[4,5] it was concluded that only when testing was carried at low temperatures, under the T_g of PP, an increase in the EC increased the capability of the material to deform plastically. At higher temperatures, the plastic deformation is limited by the PP matrix (in fact, yielding and necking cases are found in materials with low EC or without it as C1 and H0). When the EPBC plaques tested in TD direction and the ones obtained by compression molding are considered, it can be appreciated that there is no such an influence of the EC on the ductility level. All this lead us to think that the induced morphology of the skin, oriented

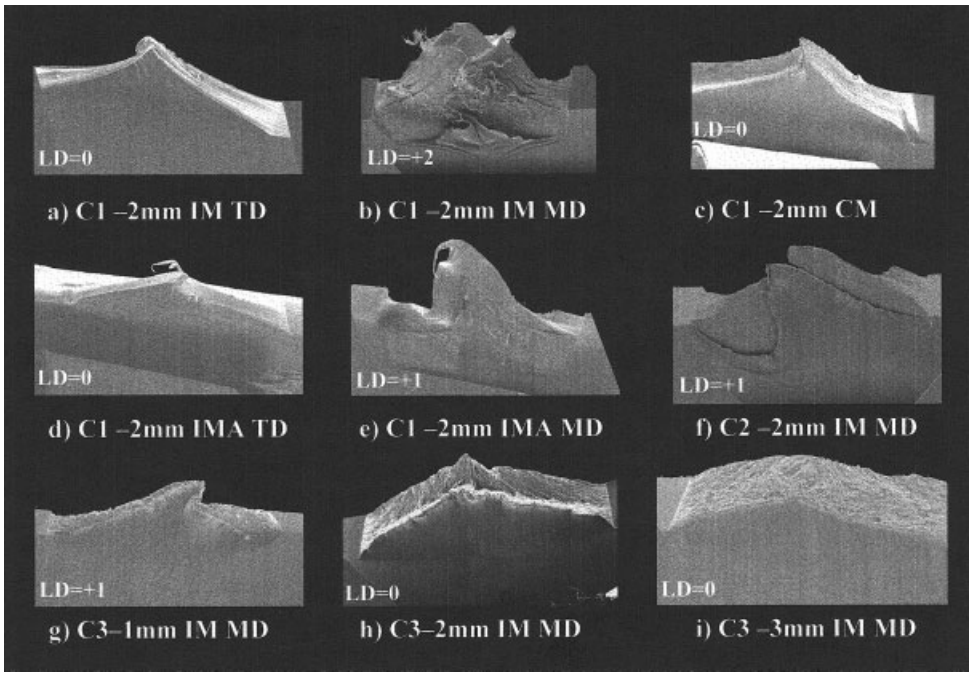

Figure 5 SEM micrographs covering all ductile fracture types.

along the MD direction, is responsible for the extreme ductile behavior of the crack tip of the injected plaques with lower EC. The increase of EC had an influence on such morphology during injection, affecting mainly on the rheological and crystallization properties of the melt, as it was shown by the DSC, WAXS, and PLM analysis done in the previous work.[2]

That reasoning can be applied to evaluate the influence on the ductility level produced by the increase of thickness in the IM-MD (Figs. 5(g)–5(i)) and IMA-MD series. However, in this case, the increase of triaxiality in the state of tension with the increase of thickness, which affects the fracture behavior, has to be considered as well.[20]

The annealing process also brought a general reduction in the ductility level in the MD direction, with a decrease of the cases presenting blunting or necking phenomena. The fractured sheets obtained by compression molding looked more alike to the TD-tested specimens than to the MD ones (Figs. 5(a), (c), and (d) and Figs. 5(b), (c), and (e)). As we get more homogeneous morphologies, with either less orientation or a lower fraction of the skin, the fracture behavior of the plaques in MD and TD directions become more alike. To find further trends and to evaluate the influence of all the variables properly, it is necessary to rely on quantitative measures of the fracture parameters. Using the EWF method, this analysis can be performed.

EWF analysis

Only the specimens that presented ductile fracture are suitable to be analyzed using the EWF method. Among these cases, when the fracture behavior fulfils the requirements previously stated, the fracture parameters w_e and βw_p are representative of the material and testing conditions. This corresponds to the samples that broke with "post-yielding" (LD = 0) fracture type, and they are the ones to which the EWF method can properly be applied. Nevertheless, the samples that showed necking and blunting also yielded good linear regression coefficients when applying the EWF technique, and these values have been included with comparative purposes. They can only be considered as indicative when analyzing how the different variables present in the study have an effect on the fracture parameters. All the values can be found in Table II.

The influence of the thickness and the testing direction on EWF parameters of the plaques depends on their processing. The plaques obtained by CM do not show significant variations of w_e and βw_p with neither the thickness nor the direction of testing, since they are free of orientation. However, in the injected plaques (IM and IMA) it can be appreciated that as the thickness increases, the differences between the values of w_e and βw_p in TD and MD are reduced.

The presence of ethylene copolymer prevented the brittle behavior of the PP homopolymer. When the EC in copolymers increases from C1 to C3, it leads to a reduction of w_e and βw_p values. This tendency is reasonable, considering that PP is able to absorb more energy than that of polyethylene in case of ductile fracture.[2–5] An increase of the volume fraction of polyethylene should come with a reduction in the energy absorbed during fracture and plastic deformation. There is, however, an exception to this trend in the

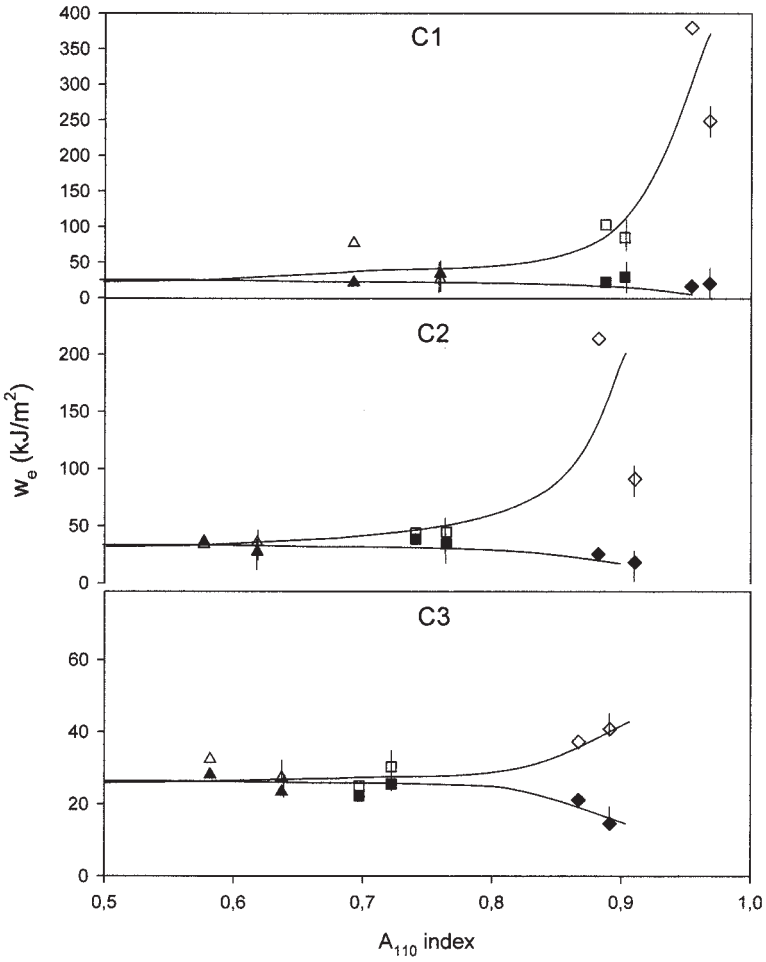

Figure 6 Dependence of the fracture parameter w_e with the orientation index A_{110}.

case of the w_e values obtained for the IM plaques tested along the TD direction, in which the material C2 presents a maximum value.

Influence of morphology

To evaluate the influence of the morphology on the fracture parameters, we can rely on the characterization made with DSC, WAXS, and PLM. In a previous work the mechanical properties of the same plaques were analyzed jointly with some morphological parameters such as crystallinity index, skin/core ratio, orientation index, and lamellar thickness.[2] When such an approach was repeated with the fracture parameters w_e and βw_p, it was found that the most significant parameters were the skin/core ratio, orientation, and crystallinity indexes.

The influence of the skin/core ratio and the orientation indexes are closely related. In general it can be said that the higher the values of skin/core ratio, the higher the different fracture behavior in MD and TD directions. CM plaques, which are free of such process-induced morphology, show uniform properties independent of the test direction. Just as the skin/core value, the orientation index A_{110} has a great influence in the anisotropy of the fracture parameters. When the values of w_e and βw_p are plotted as a function of A_{110} (as shown in Fig. 6) it can be observed that the data tend to join an asymptotic value as the A_{110} index decreases toward the nonoriented specimens. This type of representation can help to determine a representative value of the fracture parameters for a given material, regardless of the testing direction. In our case this would be 35, 30, and 25 kJ/m^2 for C1, C2, and C3, respectively. It can be noticed that values in TD do not show such a strong variation as in the case of MD specimens (although it must be kept in mind that values corresponding to blunting and necking cases are out of the prerequisites for applying the EWF method).

When the values obtained for the compression-molded plaques are added to such plots, it can be observed that in the case of material C1 they fall quite well in the predicted value. However, as the EC increases, the deviation in the fracture parameters is enhanced. In the case of C2, only the values obtained

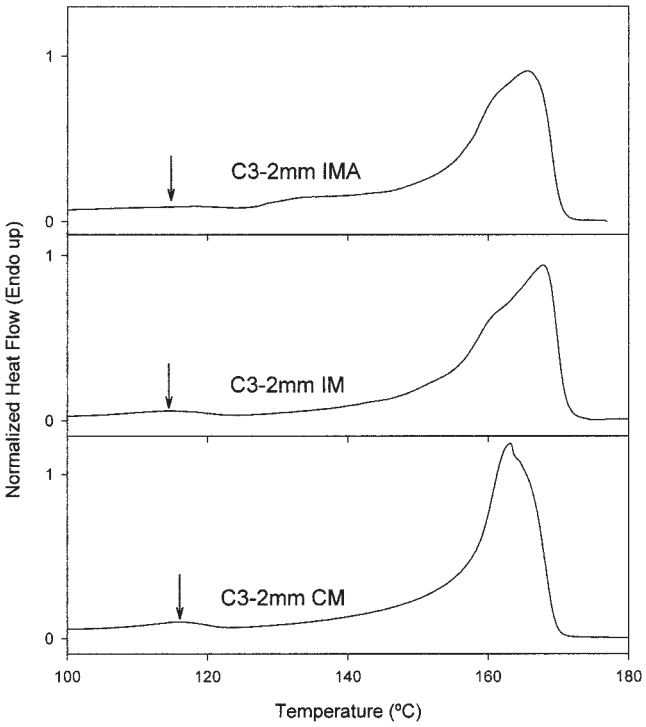

Figure 7 DSC thermograms for material C3. An arrow indicates the melting endotherm of the ethylene present as block copolymer.

for w_e are lower than what is expected and in the case of material C3 they show lower values for both w_e and βw_p parameters.

Such a behavior can be attributed to the differences in the microstructure of the plaques resulting from the different processing methods.[21,26] Since the CM process occurs with no melt shear mixing and cooling rates were lower than that in the case of the injection-molding process, it can be reasoned that the ethylene fraction of the block copolymer can present significant differences in crystallinity and the segregation state. Looking at the thermograms obtained for C3–2mm IM, C3–2mm IMA, and C3–2mm CM plaques (Fig. 7) it can be appreciated that there is a signal for the melting of the polyethylene crystals, which supports this reasoning.

Finally, a remark regarding the annealing step, which involved, in general, a raise in the crystallinity index. With respect to the fracture response of the materials, the necking and blunting cases were reduced. However, when the values tested in TD are analyzed, C1 presents a general raise of w_e and a decrease of βw_p with increasing the crystallinity index (χ_c), C2 shows a decrease of w_e but an increase in βw_p with increasing χ_c, and finally, C3 shows a reduction of w_e and βw_p when χ_c increases. Such a different evolution of toughness with crystallinity has been reviewed by Karger-Kocsis[27] and has been attributed to two opposite effects: the increase of energy absorbed by the deformation of crystalline structures and the decrease of tie molecules, which act as a stress transfer units. However, in the same work it is proposed to search for more complex models, including several variables, since many of them are interrelated.

Composite models

Another way to approach the relationships between morphology and fracture properties is by statistical analysis, using mathematical models viz. the composite model applied to the mechanical properties of the plaques, already employed in a previous work.[2] In this case, we approach the morphology skin–core–skin to a combination of three elements in parallel to describe the fracture behavior of the plaques. The thickness of the oriented skin was determined by PLM,[2] as shown in Figure 8. The total thickness (t) is the sum of the skin thickness (t_s) and the core thickness (t_c). Supposing that the fracture energies are additive and independent from each other, then:

$$W_f = W_f^{\text{skin}} + W_f^{\text{core}} + W_f^{\text{skin}} \tag{4}$$

Next, we can rewrite the eq. (1) as:

$$W_f = W_e + W_p = 2W_e^{\text{skin}} + W_c^{\text{core}} + 2W_p^{\text{skin}} + W_p^{\text{core}} \tag{5}$$

Repeating the analysis done in eq. (2) and replacing t_c by $(1-2t_s)$ we can arrive to the following expressions:

$$w_e = W_e/(lt) = w_e^{\text{skin}} \cdot 2\,t_s/t + w_e^{\text{core}} \cdot t_c/t = (w_e^{\text{skin}} - w_e^{\text{core}}) \cdot 2\,t_s/t + w_e^{\text{core}} \tag{6}$$

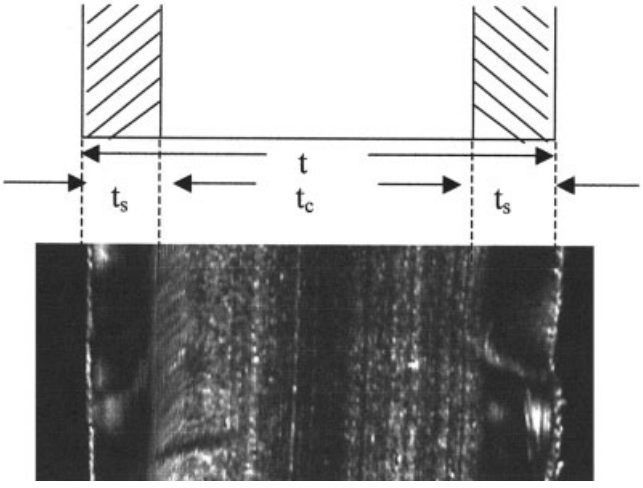

Figure 8 Sketch of the composite model (skin/core/skin) used to describe the fracture behavior of the plaques, based upon the PLM micrographs (C1–2mm IM).

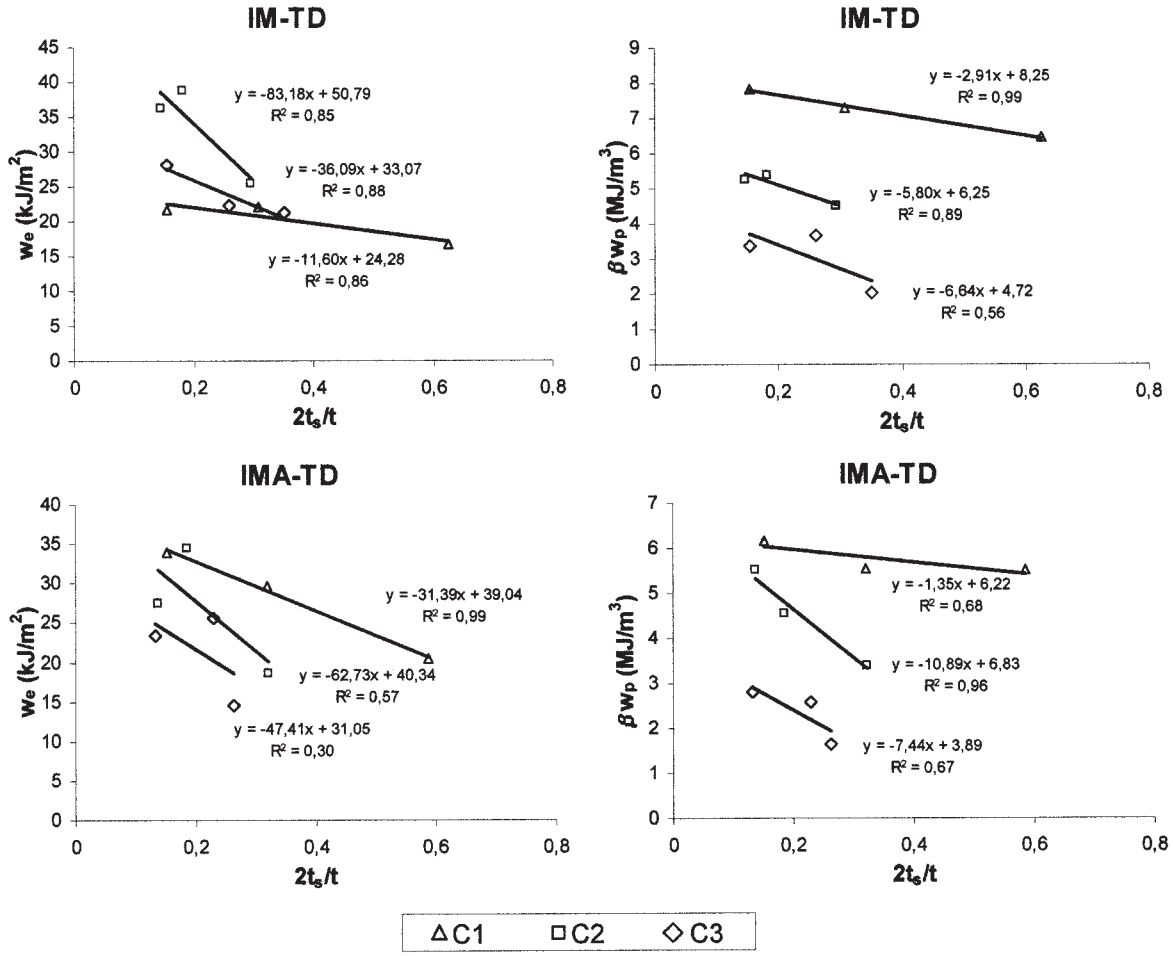

Figure 9 Application of the composite model to the fracture parameters obtained in TD.

$$\beta w_p = (\beta^{\text{skin}} w_p^{\text{skin}} - \beta^{\text{core}} w_p^{\text{core}})\, 2t_s/t + \beta^{\text{core}} w_p^{\text{core}} \tag{7}$$

From these, we can draw points of w_e and βw_p *vs.* the skin fraction ($2t_s/t$) to obtain theoretical values of fracture parameters for the skin and the core. This analysis can be performed only in the TD direction, where there are sufficient valid points, and the results are summarized in Figure 9.

It can be seen that, even if some cases yield good linear regression coefficients, the obtained values for the core do not match at all with the compression molding values, where the skin thickness is nonexistent.

This composite model could be improved using a multiple regressions statistical analysis, just as Viana and coworkers have done to study the factors involving the skin thickness in injection-molded specimens.[28] Doing so, the morphological characterization in the skin/core model can be integrated. In this new model, it should be assumed that the skin behavior is affected mainly by the A_{110} index and the core is controlled by the crystallinity index. The resulting expression should be of the form:

$$w_e, \beta w_p = f(\Sigma, X) \tag{8}$$

TABLE III
Parameters Obtained by Linear Regression of the Composite Model

	C1		C2		C3	
	w_e	βw_p	w_e	βw_p	w_e	βw_p
MD						
A			23.7	5.5	34	0
B			202	26.7	86	34.5
C			−14.5	0	−39	1.4
R^2			0.99	0.94	0.75	0.93
TD						
A	−10.6	14.7	136	8.0	98	18.1
B	21.2	−9.7	−27.1	−9.5	−88	−20.5
C	64	−11.8	−181	−3.7	−150	−29.3
R^2	0.81	0.63	0.68	0.83	0.46	0.74

$w_e = A + B^* \Sigma + C^* X$ and $\beta w_p = A + B^* \Sigma + C^* X$

In C2 MD and C3 MD only valid EWF points were used for the analysis.

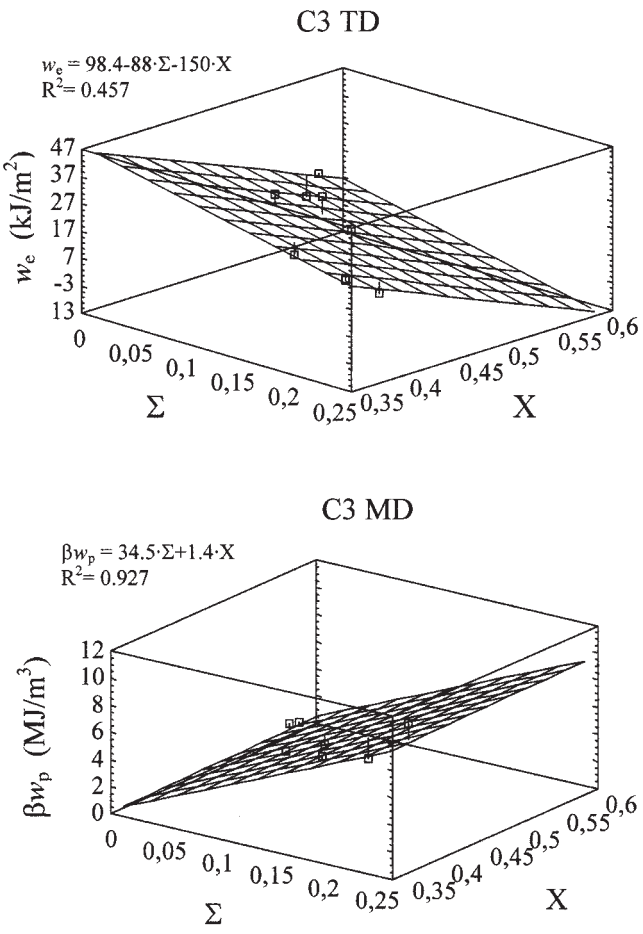

Figure 10 Application of the improved composite model using $\Sigma = A_{110} \times 2t_s/t$ and $X = \chi_c \times t_c/t$ variables, showing the plane determined by the least square regression.

Where

$$\Sigma = A_{110}\, 2\, t_s/t \tag{9}$$

and

$$X = \chi_c\, (1 - 2\, t_s/t) \tag{10}$$

Then, after plotting the fracture parameters obtained as a function of these variables, a relationship can be searched and tested by the minimum squares regression method. Arbitrarily, a linear combination of the mentioned variables has been chosen, resulting in the following results (Table III). In Figure 10, as an example, are plotted two cases with good and bad regression coefficients.

The planes defined by the equation described quite well the trends found in all cases. However, regarding the regression coefficients (Table III) it could be argued that they are not very high, indicating that either the lineal model could be revised or some other morphological variables may have an influence on the fracture response.

This model could be tested, for example, predicting the values of the CM plaques using their morphological data. This was performed for the TD direction (the only one in which all specimens could be used) and the resulting values were plotted with the data for the CM plaques (Fig. 11). Although the proposed model does not explain completely the relationships between the morphological state of the plaques and their fracture behavior, it can be seen that the trends are quite well predicted.

The sign of the coefficients obtained for Σ and X describe the combined effect of orientation and crys-

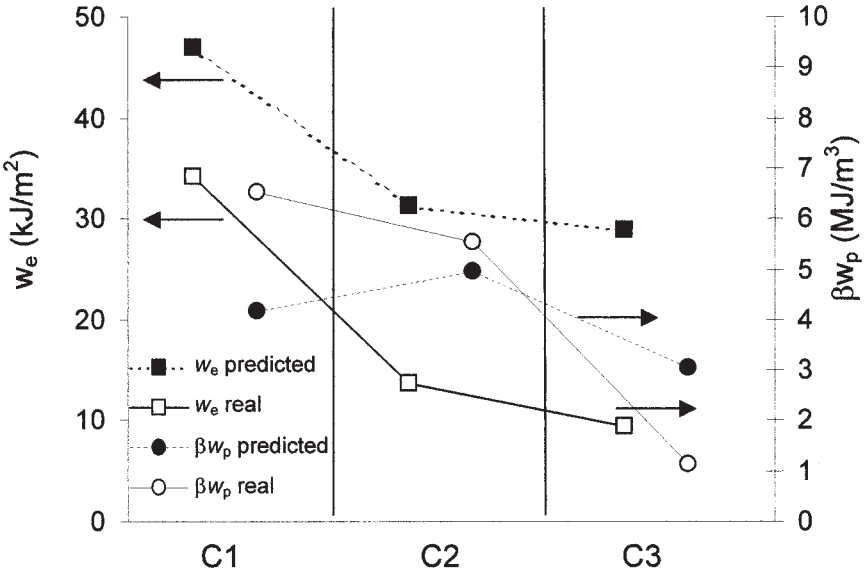

Figure 11 Application of the improved composite model to predict the fracture parameters of the CM plaques.

tallinity on the fracture behavior, depending on the testing direction. The relationships show that in MD the increase of orientation has a positive influence on toughness, and a negative influence on TD, which is in accordance with the observations done in the fractographic analysis. The increase of crystallinity index, associated to the variable X, implies in almost all cases a reduction of both w_e and βw_p parameters. This reduction of toughness is probably related to a decrease of tie molecules density.

CONCLUSIONS

The fracture behavior of thin sheets of PP and ethylene propylene block copolymers obtained by different processing methods has been studied with SEM fractographic analysis and the EWF method, considering also the influence of EC and thickness. Special emphasis has been put to the interpretation of the different fracture behavior, with the testing direction in terms of morphological parameters such as crystallinity index, orientation index, and skin–core structure. To illustrate such relationships, different models considering the skin and the core morphologies have been tested, employing the particularly useful multiple regression statistical analysis. According to the model proposed, the skin orientation has a positive influence on toughness when the direction of loading is parallel to the melt flow direction, and presents a negative influence on the transversal direction, whereas the increase of crystallinity reduced toughness in almost all cases in both testing directions.

Although the trends found explain partially the influence of several variables, which are interrelated among them, it seems necessary to continue improving a model that accounts for the morphological state of the material and its fracture properties. The use of the EWF technique has proved to be very valuable, since it provides a reliable method to characterize fracture properties of thin sheets and films.

J. Gamez-Perez is also grateful to the MCED for a doctoral grant.

References

1. Suhm, J.; Schneider, M. J.; Mülhaupt, R. In Polypropylene, an A-Z Reference; Karger-Kocsis, J., Ed.; Kluwer: Dordrecht, 1999; p 104.
2. Maspoch, M. L.; Gamez-Perez, J.; Giménez, E.; Santana, O. O.; Gordillo, A. J Appl Polym Sci 2004, 93, 2866.
3. Maspoch, M. L.; Gamez-Perez, J.; Gordillo, A.; Sánchez-Soto, M.; Velasco, J. I. Polymer 2002, 43, 4177.
4. Ferrer-Balas, D.; Maspoch, M. L.; Mai, Y.-W. Polymer 2002, 43, 3083.
5. Ferrer-Balas, D.; Maspoch, M. L.; Martínez, A. B.; Ching, E.; Li, R. K. Y.; Mai, Y.-W. Polymer 2001, 42, 2665.
6. Cotterell, B.; Reddel, J. K. Int J Fract 1977, 13, 267.
7. Broberg, K. B. J Mech Phys Solids 1975, 23, 215.
8. Mai, Y.-W.; Cotterell, B. Int J Fract 1986, 32, 105.
9. Mai, Y.-W.; Cotterell, B.; Horlyck, R.; Vigna, G. Polym Eng Sci 1987, 27, 804.
10. Mai, Y. W.; Powell, P. J Polym Sci Part B: Polym Phys 1991, 29, 785.
11. Hashemi, S. J Mater Sci 1993, 28, 6178.
12. Karger-Kocsis, J.; Czigány, T. Polymer 1996, 37, 2433.
13. Maspoch, M. L.; Santana, O. O.; Grando, J.; Ferrer-Balas, D.; Martínez, A. B. Polym Bull 1997, 39, 249.
14. Saleemi, A. S.; Nairn, J. A. Polym Eng Sci 1990, 30, 211.
15. Karger-Kocsis, J.; Czigány, T. Polym Eng Sci 2000, 40, 1809.
16. Ching, E.; Li, R. K. Y.; Mai, Y.-W. Polym Eng Sci 2000, 40, 310.
17. Hashemi, S. Polym Eng Sci 1997, 37, 912.
18. Marchal, Y.; Walhin, J. F.; Delannay, F. Int J Fract 1997, 87, 189.
19. Maspoch, M. L.; Gamez-Perez, J.; Karger-Kocsis, J. Polym Bull 2003, 50, 279.
20. Maspoch, M. L.; Ferrer, D.; Gordillo, A.; Santana, O. O.; Martinez, A. B. J Appl Polym Sci 1999, 73, 177.
21. Karger-Kocsis, J.; Mouzakis, D. E. Polym Eng Sci 1999, 39, 1365.
22. Paton, C. A.; Hashemi, S. J Mater Sci 1992, 27, 2279.
23. Wu, J.; Mai, Y. W.; Cotterell, B. J Mater Sci 1993, 28, 3373.
24. Clutton, E. In Fracture Mechanics Testing Methods for Polymers, Adhesives Composites; Moore, D. R.; Pavan, A.; Williams, J. G., Eds.; Elsevier: Oxford, 2001; p 177.
25. Hill, R. J Mech Phys Solids 1952, 1, 19.
26. Lapique, F.; Meakin, P.; Feder, J.; Jossang, T. J Appl Polym Sci 2000, 77, 2370.
27. Karger-Kocsis, J. ESIS Publication 2000, 27, 213.
28. Viana, J. C.; Cunha, A. M.; Billon, N. Polymer 2002, 43, 4185.